Inorganic Chemistry

Article

pubs.acs.org/IC

Vibronic Coupling Investigation to Compute Phosphorescence Spectra of Pt(II) Complexes

Fanny Vazart,[†] Camille Latouche,*[,†] Julien Bloino,[†,‡] and Vincenzo Barone*[,†]

[†]Scuola Normale Superiore, Piazza dei Cavalieri 7, 56126 Pisa, Italy

[‡]Consiglio Nazionale delle Ricerche, Istituto di Chimica dei Composti, OrganoMetallici (CNR-ICCOM), UOS di Pisa, Via G. Moruzzi 1, 56124 Pisa, Italy

Supporting Information

ABSTRACT: The present paper reports a comprehensive quantum mechanical investigation on the luminescence properties of several mono- and dinuclear platinum(II) complexes. The electronic structures and geometric parameters are briefly analyzed together with the absorption bands of all complexes. In all cases agreement with experiment is remarkable. Next, emission (phosphorescence) spectra from the first triplet states have been investigated by comparing different computational approaches and taking into account also vibronic effects. Once again, agreement with experiment is good, especially using unrestricted electronic computations coupled to vibronic contributions. Together with the intrinsic interest of the results, the robustness and generality of the approach open the opportunity for computationally oriented chemists to provide accurate results for the screening of large targets which could be of interest in molecular materials design.

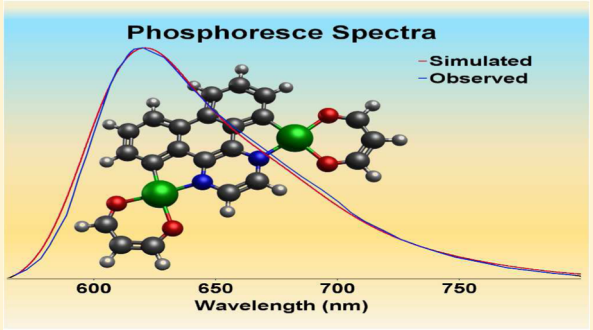

INTRODUCTION

Compounds exhibiting emission in the near-infrared are of interest for the development of organic light-emitting diodes (OLED) or light-emitting cells (LEC).[1−3] Ru(II) complexes with poly-pyridine ligands are among the most investigated organometallic and inorganic metal complexes, especially thanks to their strong ability to phosphoresce in this energy range.[4−12] In spite of this remarkable behavior, all those complexes are characterized by low quantum yields, which represent an obstacle for effective applications in technological processes. To overcome those limitations, new transition metal complexes with stronger quantum yields are being designed and studied. Platinum(II) complexes seem particularly promising candidates for their strong and tunable phosphorescence, which could be of interest in a wide spectrum of applications such as sensors or storage data, especially thanks to the possibility of emitting in the 500−800 nm range.[13−15] The emission wavelength can be tuned by decreasing the LUMO energy or by raising the HOMO energy. Other possible strategies include the decrease of the HOMO−LUMO gap by increasing the intra- and interligand conjugation[16−18] or by introducing a second metal center into the molecule.[19,20] In a recent paper,[20] a combined experimental and computational investigation was performed on the geometric and electronic structures of several mono- and dinuclear platinum(II) complexes with a square planar d^8 configuration of the metal (Figure 1). The ligands consist of one or two acetylacetonate (*acac*) moiety(ies) and a biphenylpyrimidine (**I**, **IV**) or biphenylpyrazine (**II**, **III**, **V**, **VI**) bridging fragment.

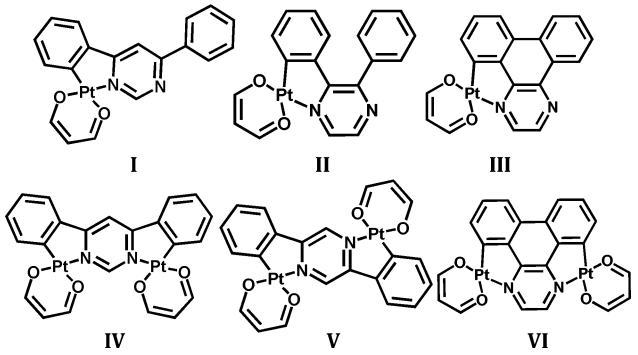

Figure 1. Compounds **I**−**VI**.

The number metal atoms and/or of ligands could allow a fine-tuning of emission wavelengths and therefore represent crucial targets to test the robustness of new computational methods. This prompted us to extend previous computational investigations (limited to electronic ground states) to emission (phosphorescence) spectra. This task is by no means trivial due to the presence of closely spaced multiplets and to the difficulty of managing triplet states by conventional methods. The dimensions (and the number) of the systems suggest the use of effective computational approaches rooted into the density functional theory (DFT) and its time-dependent extension

Received: April 3, 2015
Published: May 20, 2015

DOI: 10.1021/acs.inorgchem.5b00734
Inorg. Chem. 2015, 54, 5588−5595

Table 1. Calculated Structural Data for I–VI: Bond Lengths (Å), Angles (deg) (B3PW91/LANL2DZ+pol./PCM)

		I	II	III	IV	V	VI
Ground State	*Pt-N*	1.996	1.982	1.996	1.996	1.983	1.994
	Pt-C	1.964	1.959	1.975	1.962	1.966	1.986
	Pt-O$_1$	2.022	2.025	2.015	2.019	2.019	2.015
	Pt-O$_2$	2.128	2.144	2.127	2.128	2.134	2.115
	φ	21	55				
Triplet State (unr)	*Pt-N*	1.993	1.967	1.995	1.995	1.976	1.998
	Pt-C	1.919	1.930	1.925	1.946	1.946	1.970
	Pt-O$_1$	2.046	2.044	2.044	2.022	2.035	2.026
	Pt-O$_2$	2.113	2.142	2.104	2.119	2.133	2.101
	φ	6	42				
Triplet State (TD-DFT)	*Pt-N*	1.990	1.963	1.989	1.965 1.989	1.977	2.001
	Pt-C	1.924	1.946	1.930	1.970 1.937	1.950	1.957
	Pt-O$_1$	2.043	2.037	2.042	2.016 2.035	2.030	2.031
	Pt-O$_2$	2.123	2.148	2.113	2.143 2.133	2.135	2.108
	φ	6	37				

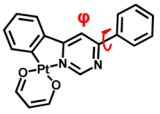

I

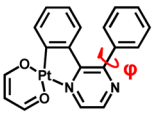

II

Table 2. Absorption Data: Experiment vs TD-DFT Calculated Values (*t* Stands for an Absorption Peak from a Singlet → Triplet Excitation (B3PW91/LANL2DZ+pol./PCM))

	λ_{exp}[a] (nm)	λ_{calcd} (nm), oscillator strength (f)	transitions involved, wt %	HO–LU gap (eV)
I	408	428 *f* = 0.09	HO → LU 85%	3.54
	338	328 *f* = 0.13	HO-3 → LU 60%	
			HO-1 → LU+1 25%	
II	449	437 *f* = 0.03	HO → LU 92%	3.59
	398	372 *f* = 0.07	HO-1 → LU 78%	
	340	356 *f* = 0.19	HO → LU+1 82%	
III	463	457 *f* = 0.04	HO → LU 93%	3.38
	407	392 *f* = 0.14	HO-1 → LU 88%	
	344	348 *f* = 0.21	HO → LU+1 89%	
IV	532sh[b]	*t* 541 *f* = 0.00	HO → LU 91%	3.24
		t 527 *f* = 0.00	HO-2 → LU 45%	
			HO-1 → LU 40%	
	481	467 *f* = 0.27	HO → LU 96%	
	430	409 *f* = 0.17	HO-2 → LU 84%	
V	618sh	*t* 628 *f* = 0.00	HO → LU 76%	3.08
	503	513 *f* = 0.12	HO → LU 95%	
	453	425 *f* = 0.24	HO-2 → LU 91%	
	372	373 *f* = 0.48	HO-6 → LU 49%	
			HO → LU+1 41%	
	333	341 *f* = 0.34	HO-2 → LU+1 87%	
VI	595sh	*t* 615 *f* = 0.00	HO-1 → LU 96%	3.05
		t 573 *f* = 0.00	HO → LU 77%	
			HO-2 → LU 13%	
	509	509 *f* = 0.10	HO → LU 91%	
	462	431 *f* = 0.25	HO-2 → LU 87%	
	428	396 *f* = 0.05	HO-5 → LU 96%	
	350	349 *f* = 0.33	HO-1 → LU+1 77%	

[a]From ref 20. [b]Shoulder.

(TD-DFT). As a matter of fact, the first triplet states of molecular systems can be considered either ground high spin electronic states (being thus amenable to standard (unrestricted) DFT computations) or excited electronic states requiring TD-DFT computations starting from the singlet ground state. A comparison between these two routes is one of the aims of the present investigation.

A second point of interest is related to geometry relaxation effects (difference between vertical and adiabatic transitions) and to vibrational modulation of electronic spectra (the so-called vibronic couplings). Thanks to the development of effective analytical derivatives for both DFT and TD-DFT methods, together with powerful and general tools for the evaluation of vibronic couplings (including Franck–Condon, Herzberg–Teller, and mode mixing effects), it has been

DOI: 10.1021/acs.inorgchem.5b00734
Inorg. Chem. 2015, 54, 5588–5595

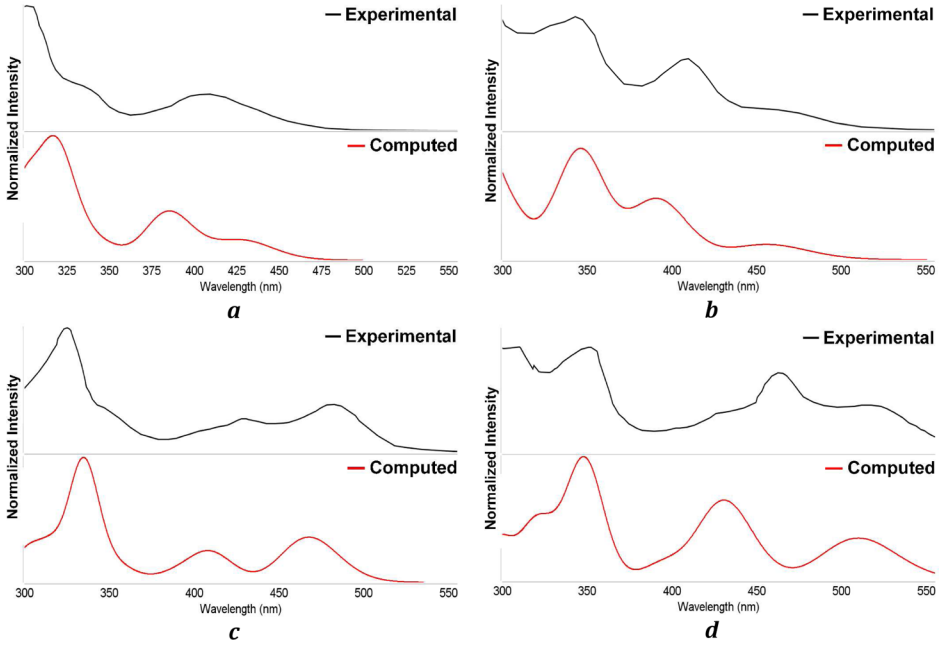

Figure 2. Experimental vs computed electronic absorption spectra of **I** (a), **III** (b), **IV** (c), and **VI** (d) (solvent included) (B3PW91/LANL2DZ +pol./PCM).

possible to perform a comprehensive investigation of those aspects which have a non-negligible impact on a proper comparison with experiments (vide infra).

Finally, in all computations, solvent effects have been taken into account by the powerful polarizable continuum model (PCM), which is fully adequate to describe general trends and even to provide quantitative results in the absence of strong and specific solute−solvent interactions (e.g., hydrogen bonds).

■ COMPUTATIONAL DETAILS

All calculations have been carried out with a development version of the Gaussian suite of program[21] using the B3PW91 hybrid density functional,[22−24] in conjunction with the LANL2DZ basis set, which includes a pseudopotential for describing inner electrons of Pt and is augmented with polarization functions on all the atoms except hydrogens (exponents equal to 0.587, 0.736, and 0.961 respectively for the *d* functions of C, N, and O and 0.8018 for the *f* function of Pt).[25−28] The choice of this couple (functional/basis set) is based on previous results pointing out the robustness of this computational model.[12,29] Solvent effects (CH_2Cl_2) were taken into account using the polarizable continuum model (PCM)[30−32] in an equilibrium regime. Full geometry optimizations have been performed for all the compounds checking the nature of the obtained structures by diagonalizing their Hessians. Excitation energies from the electronic ground state and equilibrium geometries for excited states were evaluated by means of TD-DFT and unrestricted DFT.

One-photon emission (OPE) spectra were also simulated within the Born−Oppenheimer and harmonic approximations by a time independent approach, which effectively takes into account the transitions from the ground vibrational state of the initial electronic state to all the vibrational states of the final electronic state.[33] Both vertical (same geometries for both electronic states) and adiabatic (optimized geometry for each electronic state) models were considered together with inclusion (vertical Hessian, VH, or adiabatic Hessian, AH) or not (vertical gradient, VG, or adiabatic shift, AS) of frequency changes and mode mixing between the two electronic states. In all cases, the Franck−Condon approximation was enforced, namely that the transition moment is only marginally affected by (small) geometry modifications. Further details can be found in ref 33. On the basis of test computations, the VG approach will be our standard in the following, except for some selected cases.

All of the spectra have been generated and managed by the VMS-draw graphical user interface.[34] For some specific cases, the lowest normal modes were removed from the vibronic treatment in view of their marginal role in the spectrum and poor description at the harmonic level. Composition and plot of frontier orbitals were determined respectively thanks to the Gaussview and Chemissian packages.[35,36]

■ RESULTS AND DISCUSSION

Structural Investigation. Table 1 lists some structural parameters for the fundamental singlet and first triplet states of compounds **I**−**VI**. The bond lengths (C−N, C−C, C−O) around the platinum atom are given for all compounds. For compounds **I** and **II**, the rotation of the phenyl group represented by the dihedral angle (φ), formed between the phenyl and the aza moiety, appears to be weakly hindered. Except for the possible torsion of phenyl group (which is much larger in **II** than in **I** due to the stronger hindrances it experiences in the former case) in the ground electronic state, the geometrical parameters of all the molecules are quite similar. Indeed the Pt−N distances always remain between 1.98 and 2.00 Å.

The Pt−C bond lengths have the same behavior except for complexes **III** and **VI**, which exhibit larger distances. This trend can be explained by the strong delocalization inside the ligand. Compared to the ground states, a few general trends can be observed in the excited states. In particular, one of the Pt−O bond lengths increases when going from S_0 to the triplet, whereas the other Pt−O and, especially, the Pt−C bond lengths decrease, the latter showing a stronger shortening for monometallic complexes (0.02−0.05 Å) than in the case of bimetallic ones (0.01−0.04 Å). At the same time, the φ angle decreases dramatically in the excited electronic states of **I** and **II** due to an increase of the electronic delocalization.

Absorption. TD-DFT computations have been performed at the optimized geometries of the S_0 electronic states to

DOI: 10.1021/acs.inorgchem.5b00734
Inorg. Chem. 2015, 54, 5588−5595

Table 3. Emission Data: Experiment vs TD-DFT, Unrestricted-DFT Electronic and Vibronic Calculated Values (B3PW91/LANL2DZ+pol./PCM)

		electronic		vibronic					
	exp[a]	TD-DFT	unrestricted	AS (TD)	AH (TD)	AS (unr)	AH (unr)	VG (unr)	VH (unr)
I	521	573	554	566	592	557	582	527	522
II	554	716	639	616		574		575	
	578			673		612		604	
III	568	629	609	588		575		573	
IV	558	623	571	580		552		552	
	594			628		598		599	
V	628	797	733	705		665		664	
	685			780		730		715	
VI	628	707	645	670	716	610	624	611	613

[a]From ref 20.

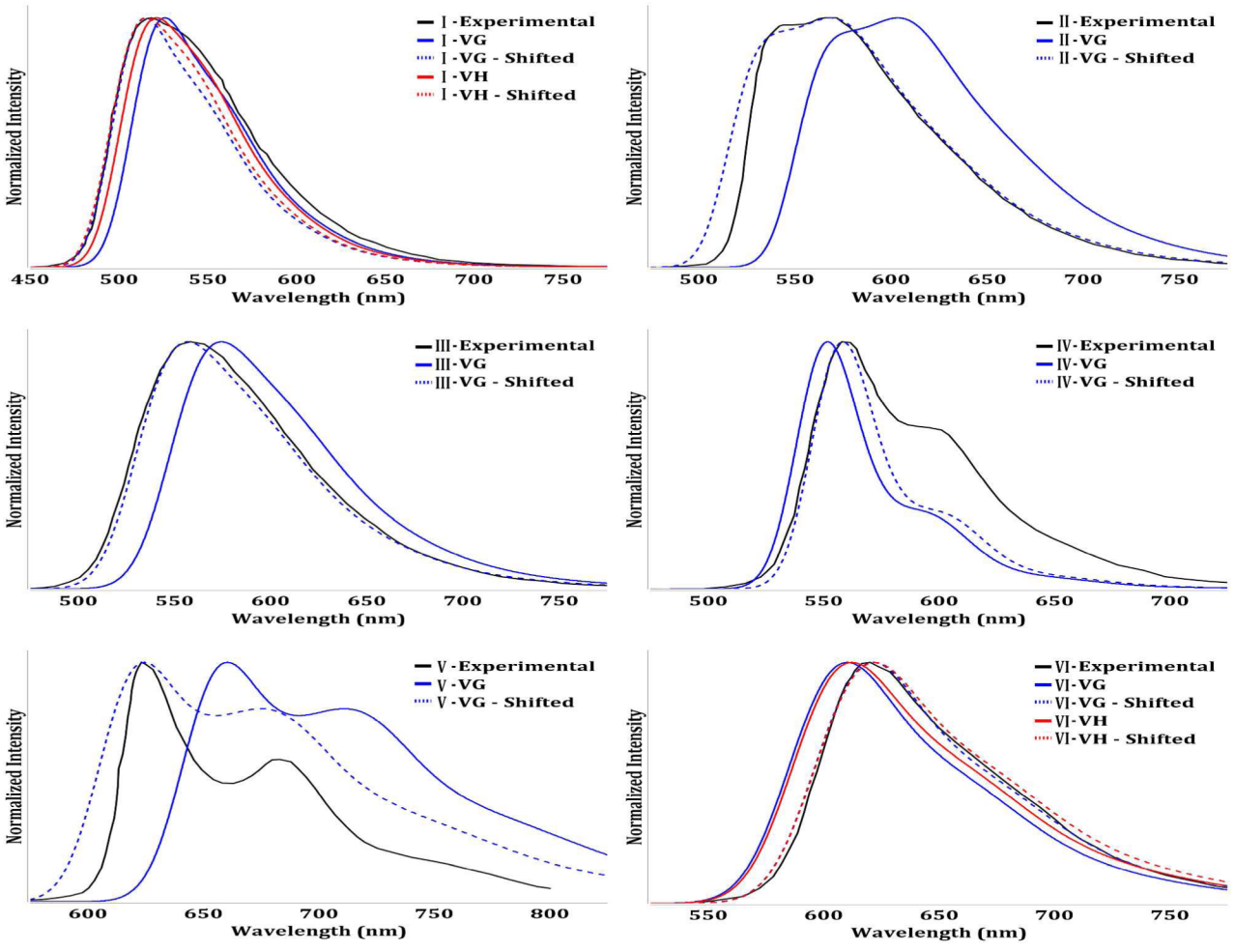

Figure 3. Experimental (black) vs simulated phosphorescence spectra at the vertical level of theory. VG (blue), VG + Shift (dashed), VH (red), VH + Shift (dashed)

investigate the absorption properties of the targeted complexes and compared to the available experimental data (Table 2, Figure 2, and Supporting Information).[20] All computed excitations are in reasonable agreement with the experimental data, confirming this computational method, in line with previous investigations.[12,29] A more detailed analysis can be based on a direct vis-à-vis comparison of the available experimental spectra[20] with those issuing from vibronic simulations. Figure 1 shows that the methodology used is robust and allows a direct vis-à-vis comparison with the

DOI: 10.1021/acs.inorgchem.5b00734
Inorg. Chem. 2015, 54, 5588−5595

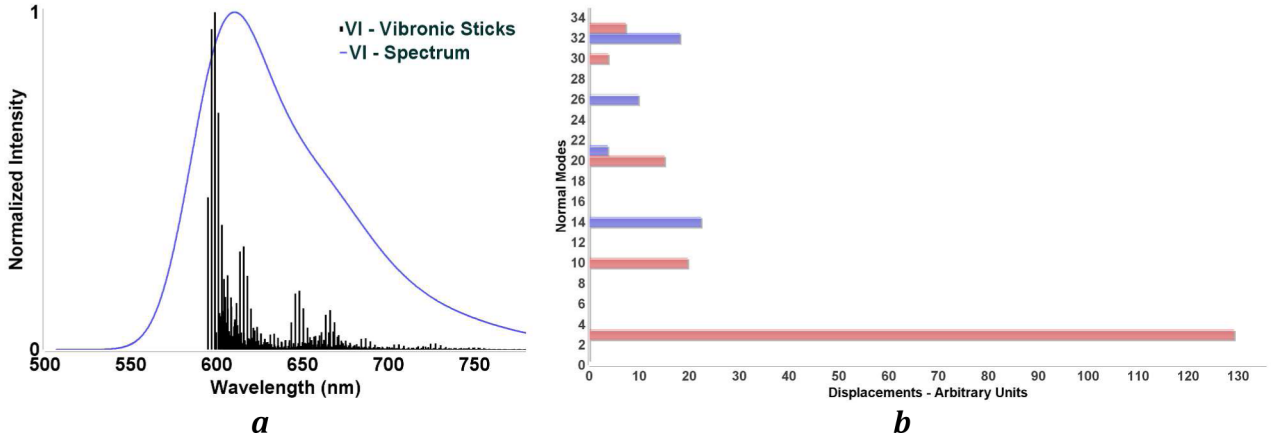

Figure 4. Stick and convoluted phosphorescence spectrum of VI (a). Main components of the shift vector along normal modes of the initial electronic state (b) (blue and red refer to positive and negative sign, respectively)

observed absorption spectra. Indeed, for all the compounds, all the absorption bands are reproduced in our simulations, and also the peak intensities match their experimental counterparts. Thanks to this accuracy, it becomes possible to assign unambiguously the absorption bands (Table 2). As already discussed in a previous paper by Williams et al,[20] the first transition is mainly a HOMO to LUMO transition with a strong metal-to-ligand charge transfer (MLCT) character. Indeed, as expected, the HOMOs involved in the transitions exhibit a strong platinum character (especially its *d* orbitals), leading to the so-called MLCT (the contributions are reported in Supporting Information). *Acac* moiety plays a negligible role in the transitions due to its marginal contributions in the frontier orbitals. The C_4N_2 ring possesses the strongest accepting ability, and therefore the LUMO and LUMO+1 of each compound are strongly localized on this moiety and, in the case of the LUMO, more precisely on both nitrogen atoms. For the bimetallic complexes, symmetry constraints impose equal contributions of both Pt atoms and both *acac* moieties in the MOs. As suggested by Williams and co-workers, a spin-forbidden transition (singlet to triplet) occurs for some biplatinum complexes and is well reproduced in our computations.[20]

However, nothing related to this singlet → triplet excitation has been discussed on **VI**, whereas, according to our computations, two excitations also appear at 615 and 573 nm. These values fit nicely with the observed tail around 600 nm in the experimental spectrum. The computed data reported in Table 2, and the simulated spectra in Figure 2 fit nicely with experimental data. One should notice that some asymmetric bands are well reproduced in our computations which involve several electronic states. Vibrational progressions, if not negligible, are thus masked by overlapping Gaussians describing the average behavior of electronic states: under such circumstances, explicit vibronic computations are of marginal interest.

Phosphorescence. The phosphorescence wavelength was first studied by conventional open-shell DFT computations (unrestricted) of the first triplet state. In this case the electronic wavelength was obtained as the energy difference between the optimized triplet open-shell ($E_{T,r(T)}$) and a single-point calculation of the singlet closed-shell with the optimized geometry of the triplet ($E_{S,r(T)}$). This method gives on average an error around 0.15 eV. While the error is higher for complexes **II** and **V**, it remains acceptable even in this case (<0.30 eV) (Table 3).

This preliminary study paves the way to more refined calculations based on vibronic transitions. As one can see in Table 3, the vibrational contributions affect the position of the peaks. In every case, the *unrestricted* method provided accurate results in term of position. Furthermore, the "cheap" AS and VG levels of theory show a substantial agreement with respect to experiment. Indeed, after inclusion of these corrections in the VG case, the average error on each peak falls around 0.06 eV with respect to experiment. Upon additions of Hessian effects, the peaks are all shifted to lower energies, with the exception of **I** (VH).

Let us now discuss the global band shape. Contrary to absorption spectra, the phosphorescence ones involve only one final electronic state (S_0), so that any asymmetry (or fine structure) in the spectral shape can only originate from vibronic effects. Figure 3 shows the overall spectra obtained by unrestricted DFT electronic computations together with VG or VH treatments of vibronic contributions. The band shape for each compound is well reproduced by our computations, giving further support to the reliability of the underlying computational approach. Indeed, it is observed that complex **II** has two intense peaks, with a difference of ca. 30 nm, and the first slightly less intense in comparison to the second one. This behavior is well reproduced by our computations. Furthermore, for complexes **III** and **VI**, experimental and observed phosphorescence spectra are almost identical. For complexes **IV** and **V**, despite a slight discrepancy on the shoulder intensity of the curve, the localization of the peak is, once again, in good agreement with experimental data. As tests cases, the band shape of **I** and **VI** have also been investigated after a Hessian diagonalization on both structures ($E_{T,r(T)}$ and $E_{S,r(T)}$). As a matter of fact, the resulting spectrum (VH) fits slightly better the experimental one.

Conventional TD-DFT computations from the S_0 ground electronic state led to larger and less systematic errors. In particular, complexes **I**, **III**, **IV**, and **VI** shared a systematic error of ca. 10%, which is quite typical for this level of theory. On the other hand, the error for **II** and **V** reached 25%, a value too high to allow any reliable investigation. If one compares the TD-DFT electronic energies with respect to the experimental ones, the disagreement is always above 0.20 eV, and up to 0.50 eV (**II**), with a mean value of about 0.30 eV (based on the highest

DOI: 10.1021/acs.inorgchem.5b00734
Inorg. Chem. 2015, 54, 5588−5595

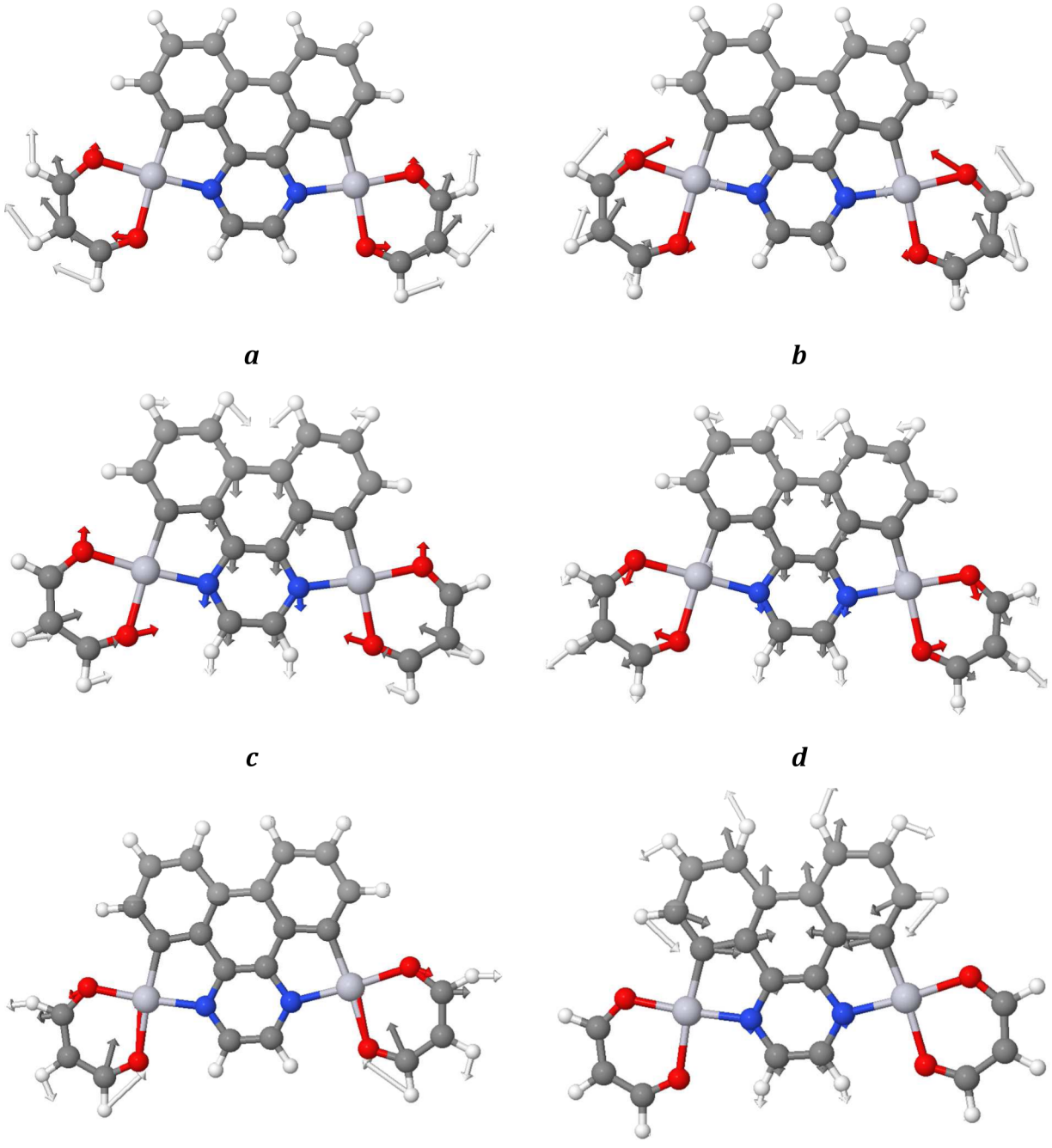

Figure 5. Normal modes 3 (a), 10 (b), 14 (c), 20 (d), 26 (e), and 32 (f) of the triplet state of **VI**.

experimental energy values). However, upon addition of the vibronic coupling, the error drops, ranging from about 0.07 to 0.30 eV, with an average around 0.20 eV. It is of interest to analyze the main normal modes ruling the vibrational progressions of the emission spectra. In Figure 4a, the simulated phosphorescence spectrum of complex **VI**, is superimposed to the stick spectrum showing the different vibrational contributions at the VG level of theory. As one can see, the band maximum does not correspond to the 0−0 transition but to excited vibrational levels. To characterize the principal vibrational progressions, the main components of the shift vector (i.e., the gradient of the final state projected on the normal modes of the initial state) is shown in Figure 4b (the projections of the shift vectors along all the normal modes are given in Supporting Information).

One can notice that the third normal mode of the triple state (unrestricted), whose computed harmonic frequency is 56 cm^{-1}, dominates the shift vector, followed by non-negligible (although at least 6 times lower) contribution by normal modes 10, 14, 20, 26, and 32, whose computed harmonic frequencies are 133, 202, 263, 361, and 455 cm^{-1}, respectively. These six modes (3, 10, 14, 20, 26, 32) are sketched in Figure 5. It is noteworthy that all of these modes involve out-of-plane displacements and receive significant contributions from the *acac* moiety. Actually, modes 3, 10, 26, and 32 involve exclusively the *acac* moiety. This point is remarkable because this moiety is only weakly involved in the electronic transition (cf. Absorption section), but contributes strongly to tune the overall band shape.

DOI: 10.1021/acs.inorgchem.5b00734
Inorg. Chem. 2015, 54, 5588−5595

CONCLUSIONS AND PERSPECTIVES

From a methodological point of view, the B3PW91 hybrid functional in conjunction with the LANL2DZ valence basis set and pseudo potential confirms its reliability and robustness for analyzing structural and spectroscopic features of transition metal complexes involving, inter alia, platinum and ruthenium, together with different kinds of conjugated ligands.[12,29] For high spin states, both conventional unrestricted DFT and TD-DFT (starting from the singlet ground state) computations can be performed with the first approach, providing more reliable results. Inclusion of vibronic couplings then leads to remarkable agreement with experiment: positions, intensities, and band shapes are nicely reproduced in our simulated spectra. It is noteworthy that the *acac* moiety gives a marginal direct contribution to the electronic transition but tunes the band shape through vibronic couplings.

These results pave the route toward new interactions between theory and experiment to design advanced molecular devices. Nevertheless, some limitations are still present especially concerning proper account of the spin−orbit coupling, which would allow the computation of absolute (instead of relative) intensities together with Herzberg−Teller effects. Recent developments in this specific area[37−39] pave the route toward more refined yet feasible computations. Another significant aspect is the proper treatment of inner electrons beyond the pseudopotential approach employed in the present work. Here again, effective relativistic models are already available or are being developed, which can be profitably used in the near future. Work is in progress along these directions in our laboratory, together with the definition and investigation of suitable benchmarks, to assess the performances of electronic and vibronic approaches in the field of large transition metal complexes in their natural environment.

ASSOCIATED CONTENT

Supporting Information

Fragments and atoms contributions to MOs (%). MO plots of the transitions involved in the absorption peaks for **I**−**VI**. Experimental vs computed absorption spectra of **II** and **V**. Singlet and triplet (by unrestricted-DFT and TD-DFT calculations) states geometric representations. Shift vector of all normal modes of complex **VI**. The Supporting Information is available free of charge on the ACS Publications website at DOI: 10.1021/acs.inorgchem.5b00734.

AUTHOR INFORMATION

Corresponding Authors

*For C.L.: E-mail, camille.latouche@sns.it.
*For V.B.: E-mail, vincenzo.barone@sns.it.

Notes

The authors declare no competing financial interest.

ACKNOWLEDGMENTS

Vincenzo Barone acknowledges the ERC project (European Research Council advanced grant 320951-DREAMS). Julien Bloino also acknowledges support from the Italian MIUR (FIRB 2012: Progettazione di materiali nanoeterogenei per la conversione di energia solare, protocollo, RBFR122HFZ).

REFERENCES

(1) D'Andrade, B. W.; Forrest, S. R. *Adv. Mater.* **2004**, *16*, 1585−1595.
(2) Sun, Y.; Forrest, S. R. *Appl. Phys. Lett.* **2007**, *91*, 263503.
(3) Chen, C.-Y.; Pootrakulchote, N.; Chen, M.-Y.; Moehl, T.; Tsai, H.-H.; Zakeeruddin, S. M.; Wu, C.-G.; Grätzel, M. *Adv. Energy Mater.* **2012**, *2*, 1503−1509.
(4) Juris, A.; Balzani, V.; Barigelletti, F.; Campagna, S.; Belser, P.; von Zelewsky, A. *Coord. Chem. Rev.* **1988**, *84*, 85−277.
(5) Bhuiyan, A. A.; Kincaid, J. R. *Inorg. Chem.* **1998**, *37*, 2525−2530.
(6) Endicott, J. F.; Chen, Y.-J. *Coord. Chem. Rev.* **2007**, *251*, 328−350.
(7) Odongo, O.; Heeg, M. J.; Chen, Y.; Xie, P.; Endicott, J. F. *Inorg. Chem.* **2008**, *47*, 7493−7511.
(8) Chen, Y.; Xie, P.; Endicott, J. F. *J. Phys. Chem. A* **2004**, *108*, 5041−5049.
(9) Tsai, C.-N.; Allard, M. M.; Lord, R. L.; Luo, D.-W.; Chen, Y.-J.; Schlegel, H. B.; Endicott, J. F. *Inorg. Chem.* **2011**, *50*, 11965−11977.
(10) Lin, J.-L.; Tsai, C.-N.; Huang, S.-Y.; Endicott, J. F.; Chen, Y.-J.; Chen, H.-Y. *Inorg. Chem.* **2011**, *50*, 8274−8280.
(11) Macatangay, A.; Endicott, J. *Inorg. Chem.* **2000**, *39*, 437−446.
(12) Latouche, C.; Baiardi, A.; Barone, V. *J. Phys. Chem. B* **2015**, DOI: 10.1021/jp510589u.
(13) Latouche, C.; Lanoë, P.-H.; Williams, J. A. G.; Guerchais, V.; Boucekkine, A.; Fillaut, J.-L. *New J. Chem.* **2011**, *35*, 2196−2202.
(14) Fillaut, J.; Akdas-Kilig, H.; Dean, E.; Latouche, C.; Boucekkine, A. *Inorg. Chem.* **2013**, *52*, 4890−4897.
(15) Savel, P.; Latouche, C.; Roisnel, T.; Akdas-Kilig, H.; Boucekkine, A.; Fillaut, J.-L. *Dalton Trans.* **2013**, *42*, 16773−16783.
(16) Okada, S.; Okinaka, K.; Iwawaki, H.; Furugori, M.; Hashimoto, M.; Mukaide, T.; Kamatani, J.; Igawa, S.; Tsuboyama, A.; Takiguchi, T.; Ueno, K. *Dalton Trans.* **2005**, 1583−1590.
(17) Lamansky, S.; Djurovich, P.; Murphy, D.; Abdel-Razzaq, F.; Kwong, R.; Tsyba, I.; Bortz, M.; Mui, B.; Bau, R.; Thompson, M. E. *Inorg. Chem.* **2001**, *40*, 1704−1711.
(18) Lepeltier, M.; Le Bozec, H.; Guerchais, V.; Lee, T. K.-M.; Lo, K. K.-W. *Organometallics* **2005**, *24*, 6069−6072.
(19) Wu, S.-H.; Burkhardt, S. E.; Yao, J.; Zhong, Y.-W.; Abruña, H. D. *Inorg. Chem.* **2011**, *50*, 3959−3969.
(20) Culham, S.; Lanoë, P.-H.; Whittle, V. L.; Durrant, M. C.; Williams, J. A. G.; Kozhevnikov, V. N. *Inorg. Chem.* **2013**, *52*, 10992−11003.
(21) Frisch, M. J.; Trucks, G. W.; Schlegel, H. B.; Scuseria, G. E.; Robb, M. A.; Cheeseman, J. R.; Scalmani, G.; Barone, V.; Mennucci, B.; Petersson, G. A.; Nakatsuji, H.; Caricato, M.; Li, X.; Hratchian, H. R.; Izmaylov, A. F.; Bloino, J.; Zheng, G.; Sonnenberg, J. L.; Hada, M.; Ehara, M.; Toyota, K.; Fukuda, R.; Hasegawa, J.; Ishida, M.; Nakajima, T.; Honda, Y.; Kitao, O.; Nakai, H.; Vreven, T.; Montgomery Jr. J. A. Peralta, J. R.; Ogliaro, F.; Bearpark, M.; Heyd, J. J.; Brothers, E.; Kudin, K. N.; Staroverov, V. N.; Kobayashi, R.; Normand, J.; Raghavachari, K.; Rendell, A.; Burant, J. C.; Iyengar, S. S.; Tomasi, J.; Cossi, M.; Rega, N.; Millam, J. M.; Klene, M.; Knox, J. E.; Cross, J. B.; Bakken, V.; Adamo, C.; Jaramillo, J.; Gomperts, R.; Stratmann, R. E.; Yazyev, O.; Austin, A. J.; Cammi, R.; Pomelli, C.; Ochterski, J. W.; Martin, R. L.; Morokuma, K.; Zakrzewski, V. G.; Voth, G. A.; Salvador, P.; Dannenberg, J. J.; Dapprich, S.; Daniels, A. D.; Farkas, O.; Foresman, J. B.; Ortiz, J. V; Cioslowski, J.; Fox, D. J. *Gaussian 09*; Gaussian, Inc.: Wallingford, CT, 2014; *GDVH37p*.
(22) Becke, A. D. *J. Chem. Phys.* **1993**, *98*, 5648−5652.
(23) Perdew, J. P. *Phys. Rev. B* **1986**, *33*, 8822−8824.
(24) Perdew, J. P.; Burke, K.; Wang, Y. *Phys. Rev. B* **1996**, *54*, 16533−16539.
(25) Dunning, T. H.Jr.; Hay, P. J. In *Methods of Electronic Structure Theory SE-1*; Schaefer, H., III, Ed.; Modern Theoretical Chemistry; Springer New York, 1977; Vol. 3, pp 1−27.
(26) Hay, P. J.; Wadt, W. R. *J. Chem. Phys.* **1985**, *82*, 270−283.
(27) Hay, P. J.; Wadt, W. R. *J. Chem. Phys.* **1985**, *82*, 299−310.
(28) Wadt, W. R.; Hay, P. J. *J. Chem. Phys.* **1985**, *82*, 284−298.
(29) Baiardi, A.; Latouche, C.; Bloino, J.; Barone, V. *Dalton Trans.* **2014**, *43*, 17610−17614.
(30) Barone, V.; Cossi, M.; Tomasi, J. *J. Chem. Phys.* **1997**, *107*, 3210.

DOI: 10.1021/acs.inorgchem.5b00734
Inorg. Chem. 2015, 54, 5588−5595

(31) Cossi, M.; Scalmani, G.; Rega, N.; Barone, V. *J. Chem. Phys.* **2002**, *117*, 43.
(32) Tomasi, J.; Mennucci, B.; Cammi, R. *Chem. Rev.* **2005**, *105*, 2999−3094.
(33) Bloino, J.; Biczysko, M.; Santoro, F.; Barone, V. *J. Chem. Theory Comput.* **2010**, *6*, 1256−1274.
(34) Licari, D.; Baiardi, A.; Biczysko, M.; Egidi, F.; Latouche, C.; Barone, V. *J. Comput. Chem.* **2015**, *36*, 321−334.
(35) Dennington, R.; Keith, T.; Millam, J. *GaussView*, version 5; Semichem Inc.: Shawnee Mission, KS, 2009.
(36) Skripnikov, L. *Chemissian, A Computer Program to Analyse and Visualise Quantum-Chemical Calculations*, 2012.
(37) Brahim, H.; Daniel, C.; Rahmouni, A. *Int. J. Quantum Chem.* **2012**, *112*, 2085−2097.
(38) Gourlaouen, C.; Daniel, C. *Dalton Trans.* **2014**, *43*, 17806−17819.
(39) Brahim, H.; Daniel, C. *Comput. Theor. Chem.* **2014**, *1040−1041*, 219−229.

DOI: 10.1021/acs.inorgchem.5b00734
Inorg. Chem. 2015, 54, 5588−5595